

The Interfacial Effect on the Open Circuit Voltage of Ionic Thermoelectric Devices with Conducting Polymer Electrodes

Saeed Mardi, Dan Zhao, Nara Kim, Ioannis Petsagkourakis, Klas Tybrandt, Andrea Reale, and Xavier Crispin*

Organic-based energy harvesting devices can contribute to a sustainable solution for the transition to renewable energy sources. The concept of ionic thermoelectrics (iTE) has been recently proposed and motivated by the high values of thermo-voltage in electrolytes. So far, most research has focused on developing new electrolytes with high Seebeck coefficient. Despite the major role of the electrode materials in supercapacitors and batteries, the effect of various electrodes on energy harvesting in iTE devices has not been widely studied. In this work, the conducting polymer poly(3,4-ethylenedioxythiophene):poly-styrene sulfonate (PEDOT:PSS) is investigated as the functional electrodes in iTE supercapacitors. Through investigating the thermo-voltage of iTEs of the same electrolyte with varying composition of PEDOT electrodes, it is identified that the different PSS content greatly affects the overall thermo-induced voltage coefficient, S_{eff} (i.e., effective thermopower). The permselective polyanion in the electrode causes cation concentration differences at the electrode/electrolyte interface and contributes to an interfacial potential drop that is temperature dependent. As a result, the overall thermo-voltage of the device possesses both an interfacial and a bulk contribution. The findings extend the fundamental understanding of iTE effect with functional electrodes, which could lead a new direction to enhance the heat-to-electricity conversion.

of the energy source used in society is transformed into thermal energy.^[2] Due to the distributed nature of heat sources and low-temperature differential, about 50% of the thermal energy below 150 °C is wasted.^[3] Technologies such as organic Rankine cycles,^[4] thermo-osmotic energy conversion systems,^[5] and thermoelectric generators can harvest energy from low temperature heat sources.^[6] Among them, thermoelectric-based energy harvesting devices are attractive because of their simple structure, and non-moving parts operation; but, they are typically expensive because of the exotic materials and a tedious manufacturing process.

There are three types of thermoelectric harvesting devices, including the electronic thermoelectric devices,^[7] the thermogalvanic cells (TGC),^[8] and the ionic thermoelectric devices. The last category is based on the ionic Seebeck effect where the ions are not electroactive. The thermodiffusion of ions (also called Soret effect)^[9] under a temperature gradient can result in a large

thermo-voltage between the cold and hot electrodes (the ratio between the generated open circuit voltage (ΔV) and the applied temperature difference (ΔT) is called ionic Seebeck coefficient). Various electrolytes of high ionic Seebeck coefficient and good ionic conductivity have been reported.^[10–12] In contrast to electronic materials, the thermodiffused ions cannot pass through the electrode. Instead, these ions accumulate at the electrolyte/electrode interface and form an electric double layer capacitor (EDLC) on the electrode.^[9,13] Hence, this ionic thermoelectric effect can be used to charge a supercapacitor or a battery. The ionic thermoelectric supercapacitor/battery (ITESC) concept differs from the generators (TEG and TGC) in that it does not produce constant power versus time, since once the electrodes are charged, the power becomes zero. The ITESC can be discharged when the applied temperature gradient changes. Hence, ITESCs are relevant for intermittent heat sources, like the sun. One of the attractive features of ITESC is the use of low-cost organic polymer electrolytes, which are compatible with low-cost manufacturing techniques such as printing and dispensing technologies. This constitutes a major advantage for mass-implementation of a new energy technology.


An ITESC of capacitance C is equivalent to a TEG or a TGC in series with a capacitor of the same capacitance.^[9] Hence,

1. Introduction

Sustainability including good management of energy resources is a key topic for the transition from fossil energy sources (still 85% worldwide) to renewable energy sources.^[1] About 60%

S. Mardi, D. Zhao, N. Kim, I. Petsagkourakis, K. Tybrandt, X. Crispin
Laboratory of Organic Electronics (LOE)
Department of Science and Technology
University of Linköping
Bredgatan 34, Norrköping 581 83, Sweden
E-mail: xavier.crispin@liu.se

S. Mardi, A. Reale
Centre for Hybrid and Organic Solar Energy (CHOSE)
Department of Electronic Engineering
University of Rome Tor Vergata
via del Politecnico 1, Rome 00133, Italy

 The ORCID identification number(s) for the author(s) of this article can be found under <https://doi.org/10.1002/aelm.202100506>.

© 2021 The Authors. Advanced Electronic Materials published by Wiley-VCH GmbH. This is an open access article under the terms of the Creative Commons Attribution-NonCommercial-NoDerivs License, which permits use and distribution in any medium, provided the original work is properly cited, the use is non-commercial and no modifications or adaptations are made.

DOI: 10.1002/aelm.202100506

electronic thermoelectric materials in a TEG-C or redox electrolytes in a TGC-C series circuit can be compared in a fair fashion to an ITESC. The performance of an ionic thermoelectric material can be described through the figure of merit

$$ZT = \frac{S^2 \sigma}{k} \quad (1)$$

in which S is the ionic Seebeck coefficient, σ is the ionic conductivity and κ is the thermal conductivity.^[14] The high ionic Seebeck coefficient of electrolytes compared to the electronic Seebeck coefficient in semiconductors is attractive since the goal is to charge an energy storage device by the heat flow. Indeed, the stored electrical energy quadratically increases with the Seebeck coefficient according to:

$$E = 1/2C (\Delta T)^2 \quad (2)$$

So far, most of the researches focus on developing the electrolytes to enhance the magnitude^[10,11,15] and tuning the sign of the ionic Seebeck coefficient in devices using metal electrodes.^[16,17] However, in order to enhance the energy stored in the ITESCs, electrodes with high capacitance are required.^[18,19] A known family of materials with large specific capacitance is conducting polymers. Conducting polymer electrodes are designed to transport both electrons and ions. For that purpose, a good strategy is to consider a heterogeneous blend of an positively doped conducting π -conjugated polymer and negatively charged ionic polyelectrolyte,^[20] such as poly(3,4-ethylenedioxythiophene) composited with polystyrenesulfonate (PEDOT:PSS).^[20,21] PEDOT:PSS has been used as in various electrochemical devices such as transistors, electrochromic displays, actuators, supercapacitors, batteries, ion-pumps and sensors.^[21,22] Although PEDOT:PSS has been abundantly studied, its interface with an electrolyte is still not well understood. Recent studies have shown that conducting polymers such as polyaniline and PDAQ-BC^[23,24]

function well as electrodes in ionic thermoelectric charged supercapacitors.

In this study, we explore the role of the electrode/electrolyte interface in ionic thermoelectric supercapacitors based on an ionic gel electrolyte. By gradually tuning the composition of the electrode (PEDOT/PSS ratio), we identified that the ionic permselectivity of the polyanion PSS in the electrode composition induces a significant interfacial effect in iTE devices. Our work shows that in those ITESCs, the overall thermo-voltage is dominated by the interfacial effect, whose magnitude can be controlled by the polyanion density at the electrode surface. This work extends the understanding of the working mechanisms in ionic thermoelectric devices and suggests a new approach to improve energy conversion in thermally-chargeable supercapacitors for low-grade heat conversion applications.

2. Result and Discussion

To investigate the effect of the concentration of the polyelectrolyte PSS in the electrode, we considered the following series of electrodes made of (Figure 1a): PSSH film ($\approx 1-2 \mu\text{m}$ thick) coated on Au (PSS/Au), PEDOT:PSS films ($\approx 1-2 \mu\text{m}$ thick), post-treated with various solvents to reduce the PSS content; and PEDOT:Tos films. The first electrode made of Au coated with PSSH can be considered as having the maximum PSS surface content (100% of PSS). The second electrode is prepared from mixing commercial aqueous dispersion of PEDOT:PSS ($w_{\text{PSS}}/w_{\text{PEDOT}} = 2.5:1$) with 3 vol% of dimethyl sulfoxide (DMSO) in the water dispersion. Note that the silane agent (3-glycidoxypropyl)trimethoxysilane (GOPS) was used to cross-link the PEDOT:PSS film to prevent its dissolution in contact with polar solvents.^[25] The percentage of PSS in PEDOT could be tuned through different treatments of pristine PEDOT:PSS (without pre-added DMSO nor GOPS) with DMSO, methanol, and H_2SO_4 to remove PSS to different degrees.^[26] This allows us to obtain three PEDOT:PSS electrodes with different PSS

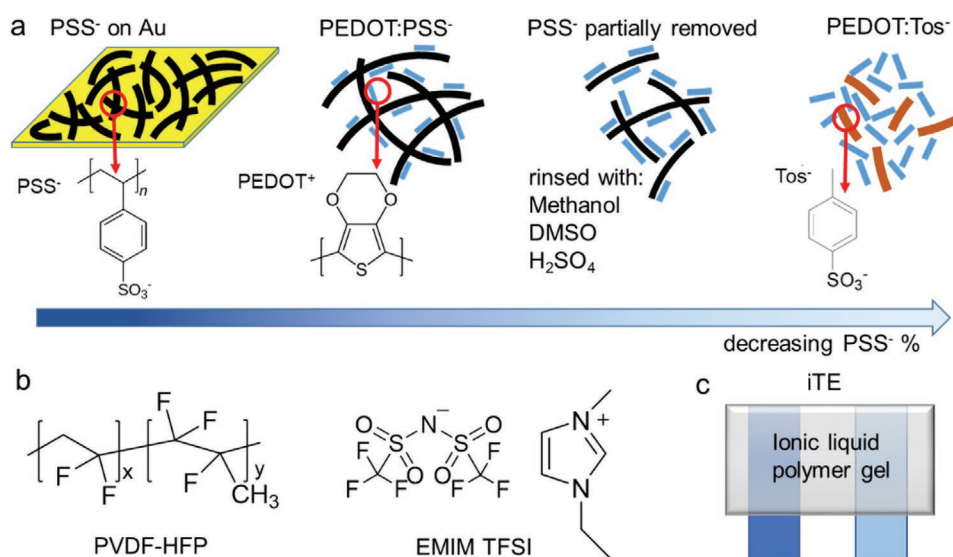


Figure 1. a) The schematic of the chemical compositions of the electrodes containing gradually decreasing amount of polyelectrolyte PSS. b) The chemical structure of electrolytes used in this study. c) The illustration of the iTE device.

contents. The last type of sample is PEDOT:Tos with a molecular anion instead of the polyanion PSS. PEDOT:Tos is composed of high density of conducting PEDOT chains packed in a paracrystalline structure. When PEDOT:Tos is in contact with an electrolyte, it is known that there is an anion exchange between the tosylate anion leaving the electrode and the anion from the solution.^[27] We expect that the highly charged PSS selectively facilitates the transport of cation and excludes the presence of anions (Donnan exclusion). Hence tuning the amount of PSS on the surface of the PEDOT electrode is expected to lead to an interfacial Donnan potential when the PEDOT electrodes are in contact with the electrolyte. The electrolyte chosen is an ionic liquid-polymer gel (IL-p gel) composed of 1-Ethyl-3-methylimidazolium bis(trifluoromethylsulfonyl)imide (EMIM-TFSI) and Poly(vinylidene fluoride-co-hexafluoropropylene) (PVDF-HFP) copolymer (with the 80 wt% of IL loading) (Figure 1b) that can be coated as a film covering the two electrodes of the ITESC (as shown in Figure 1c). This IL-p gel was previously investigated as ionic thermoelectric material for temperature sensing applications.^[16] The IL-p gel has several advantages for being the electrolyte in an ionic thermoelectric device: solution processibility, high thermal stability up to 300 °C, non-volatile (water free), low thermal conductivity ($0.136 \text{ W m}^{-1} \text{ K}^{-1}$), sufficient ionic conductivity ($\approx 2.5 \text{ mS cm}^{-1}$) and devoid of liquid leakage.^[16] Importantly, in this IL-p gel, more than 95% of IL form neutral ion pairs, so about 5% of the ions are free charged ions involved in the electrical transport.^[16] Hence, while Donnan potential at polyelectrolyte membrane typically vanishes for high ionic concentration,^[28] the IL-p gel is expected to encounter some non-negligible Donnan potential since only a fraction of the ions is not forming neutral ion-pairs. The prepared IL-p gel film can be cut and directly mounted on the electrodes, which are separated by a fixed distance (1 mm) (Figure 1c). We first investigate the stability of PSS in the electrode when in contact with the ionic liquid (IL). UV-Vis spectroscopy is used to characterize the PEDOT:PSS films before and after dipping in IL. As shown in Figure S1 (Supporting Information), the intensity of the absorption peaks from the aromatic rings of PSS^[29] remains unchanged before and after dipping in IL, indicating a rather stable interface without dissolution of PSS. When the IL-p gel is sandwiched between two PEDOT electrodes, the softness and local fluidity of the IL-p gel ensures a good ionic contact between the PEDOT electrode and the IL-p gel. This is demonstrated in the cyclic voltammogram (CV) in Figure S2 (Supporting Information). With a gold current collector underneath the PEDOT:PSS electrode, the I - V characteristics resemble a slightly distorted square box, which corresponds to a circuit composed of a resistance ($I = V/R$) in series with an ideal capacitor ($I = CdV/dt$). The I - V characteristics are very similar for PEDOT:PSS with different contents of DMSO and indicate that the PEDOT:PSS/electrolyte interface is stable and ions of the IL-p gels can penetrate into the PEDOT:PSS layer (Figure S2, Supporting Information). The CV measurements at different scan-rates (Figure S3a, Supporting Information) display a current level linearly proportional to the scan rate, as expected from a capacitive behavior. The galvanostatic charge-discharge (Figure S3b, Supporting Information) is characterized by nearly triangular shape with small IR drops, confirming the ideal capacitive properties with good electrochemical reversibility

for both electrodes.^[30] The areal capacitances were calculated from the GCD curves (Equation (7)). The calculated areal capacitances are 7.6, 8.0, and 8.4 mF cm^{-2} at the current densities of 49, 24.5, and $12.2 \mu\text{A cm}^{-2}$, respectively. In addition, the ionic conductivity of same sample was examined by the electrochemical impedance spectroscopy (EIS). Bode impedance and phase angle plots were shown in Figure S2c (Supporting Information). The ionic conductivity extracted from those impedance data was about 2.3 mS cm^{-1} (Equation (8)). This is in agreement with other reported values for this ionic gel^[16] and high enough to guarantee stable and easy thermo-voltage measurements.

As shown in Figure 1c, each device is composed of two similar electrodes connected by a free-standing deposited IL-p gel layer. The temperature gradient between two electrodes is applied and recorded synchronously with the open-circuit voltage versus time. The effect of electrical conductivity of PEDOT electrodes to the thermo-induced voltage is investigated (details can be found in Figure S4 and Note S1, Supporting Information). The good conductivity of all the PEDOT electrodes used in this study ensures that the resistive potential drops are negligible and do not affect the accuracy of the thermo-induced voltage. The thermoelectric characterization of the devices with the aforementioned electrodes and electrolyte is displayed in Figure 2. The thermo-voltage of all the devices with different ΔT are summarized in Figure 2a. The thermo-voltage increases linearly with ΔT but displays a non-ideal spurious voltage at $\Delta T = 0$ possibly attributed to non-identical electrolyte-electrode interfaces. The device with PSS/Au has the highest thermo-voltage for the same ΔT and yield a thermo-induced voltage coefficient (also called effective thermopower S_{eff}) of -4.6 mV K^{-1} (Figure 2b). Among all PEDOT electrodes, PEDOT:PSS mixed with DMSO shows the highest thermo-voltage (Figure 2c) with a S_{eff} of -3.8 mV K^{-1} . The devices with post-treated PEDOT:PSS electrodes (Figure 2d-f) all show lower thermo-induced voltage compared to the pristine one. The one treated by H_2SO_4 possesses the lowest S_{eff} of -0.9 mV K^{-1} (Figure 2f). The thermo-voltage of the device with PEDOT:Tos electrodes without polyanion is even lower than any of the PEDOT:PSS devices (Figure 2g), with a S_{eff} of only -0.8 mV K^{-1} . These results suggest that PSS indeed plays an important role in determining the thermoelectric response of the iTE devices. The trend of the thermo-induced voltage coefficient of the ITESC composed of different electrodes is consistent with our assumption, in which the thermo-voltage is dominated by the PSS/electrolyte interface potential.

The removal of PSS content from the polymer leads to the compositional and morphological changes. Previous studies have shown that the PEDOT chains are more interconnected after the treatment with H_2SO_4 and other solvents (DMSO, methanol) which leads to higher electrical conductivity.^[29,31,32] To further correlate the thermo-voltage of the ITESC devices with the content of PSS polyanion, we quantitatively analyzed the percentage of PSS in the PEDOT electrodes using UV-Vis absorption spectra normalized to 900 nm. The spectra (Figure 3a) display two absorption peaks at 192 and 226 nm from the aromatic rings of PSS and a NIR absorption background due to the free charge carriers in PEDOT. The percentage of the PSS contents in the PEDOT electrodes can be

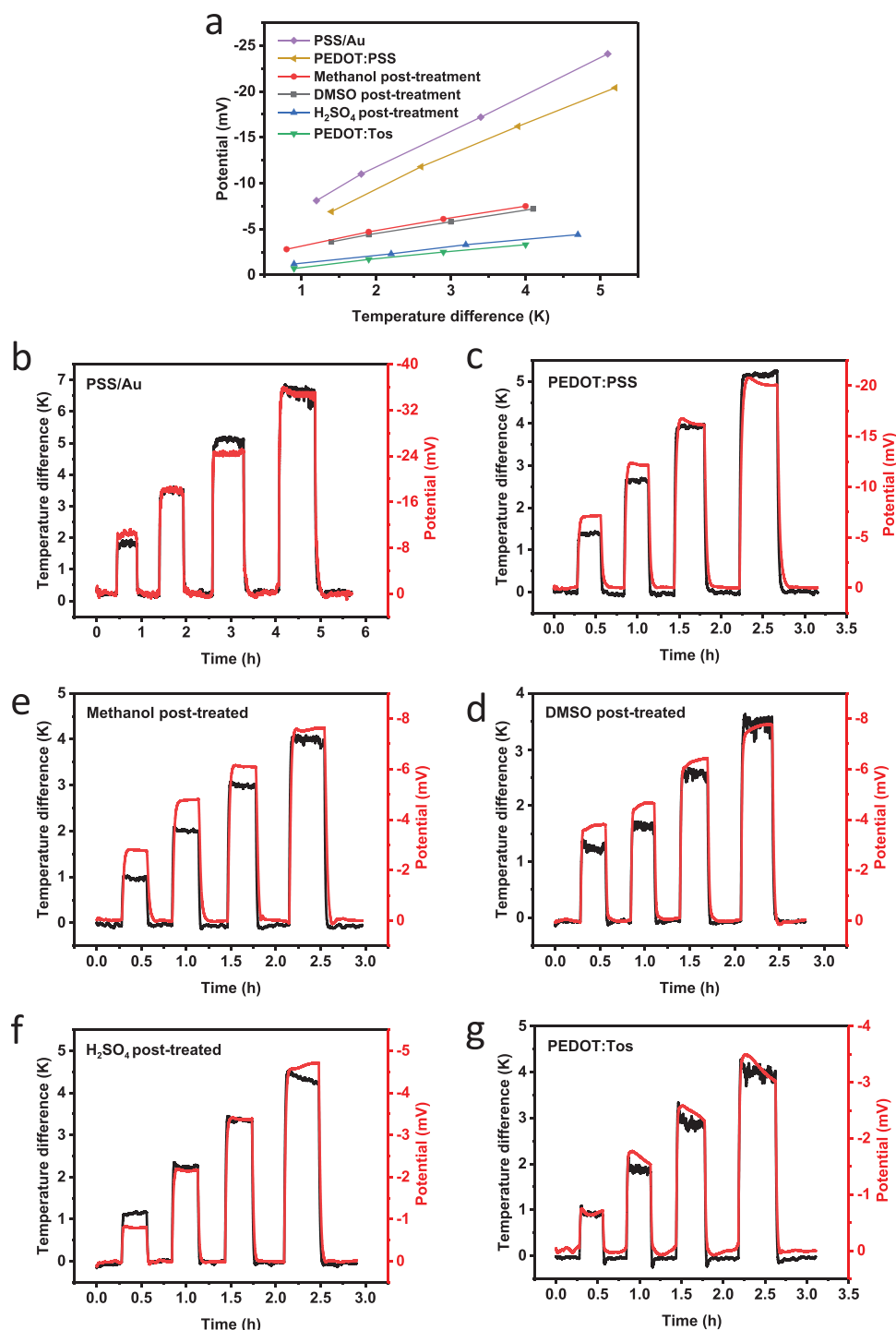


Figure 2. a) The summary of the increasing thermo-voltage with temperature difference (from 0 to 5 K) for different electrodes. Time dependence of the thermo-voltage following the applied temperature gradient steps for b) PSS/Au, c) PEDOT:PSS mixed with DMSO, post treated PEDOT:PSS with d) methanol, e) DMSO and f) H₂SO₄, g) PEDOT:Tos.

calculated by the correlation between the absorption changes at 192 nm and weight ratio of PEDOT:PSS.^[32] The PSS contents in different PEDOT:PSS is the highest in pristine PEDOT:PSS, followed by methanol-treated samples and DMSO-treated samples, and the lowest in H₂SO₄-treated ones (details can be found

in the Note S2, Supporting Information). The weight ratio of $w_{\text{PSS}}/w_{\text{PEDOT}}$ in pristine PEDOT:PSS is 1/2.5 which is equivalent to the 71% of PSS. Upon the treatment with H₂SO₄ the percentage of PSS decreased to 18%. PSS/Au and PEDOT:Tos are considered to have 100% and 0% of PSS. As shown in Figure 3b

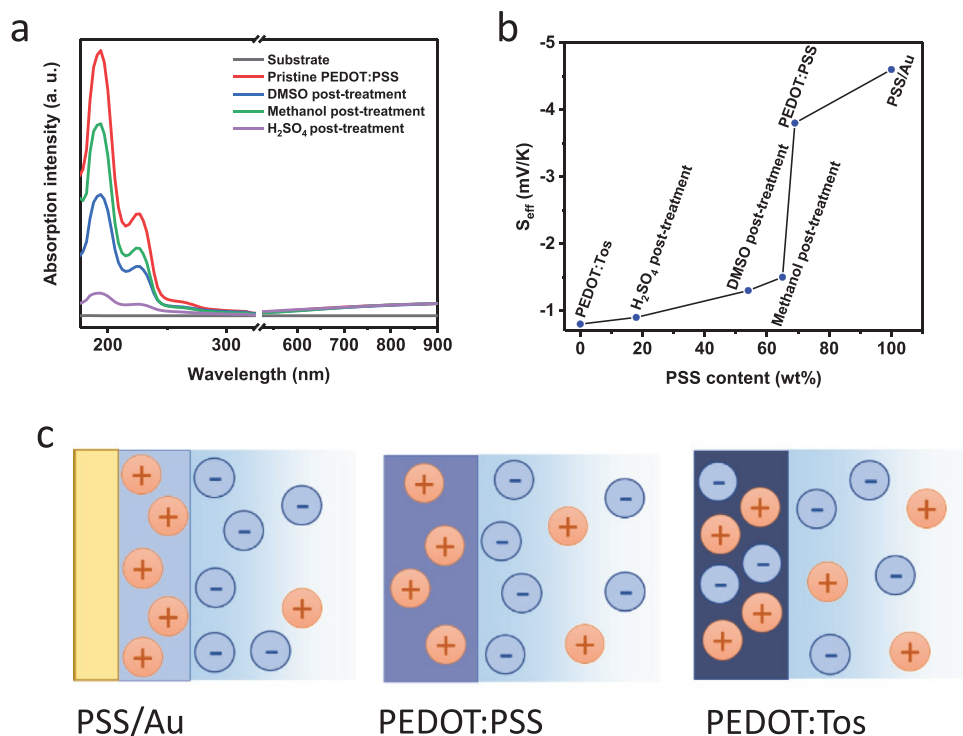


Figure 3. The correlation between the thermo-induced voltage and the PSS content in the electrodes. a) UV vis spectra of PEDOT:PSS with different PSS contents. b) The thermo-induced voltage coefficient of devices composed of different electrodes with increasing PSS contents. c) Illustration of the charge distribution at the electrode/electrolyte interface.

the magnitude of the thermo-voltage increases with PSS content. Devices with PSS/Au has the highest thermo-induced voltage coefficient, and PEDOT:Tos has the lowest. The thermo-induced voltage coefficient of the post-treated PEDOT:PSS decreases dramatically compared to the pristine PEDOT:PSS. This observation proves that the PSS induces a Donnan-like potential which significantly affects thermo-voltage in the ITESCs with PEDOT electrodes (as illustrated in Figure 3c).

The thermo-voltage of an ionic thermoelectric device operated under a ΔT can be expressed as a sum of two contributions.^[18] The first part is a result of the thermodiffusion of ions in the bulk of the electrolyte along the temperature gradient. The second term is the temperature-dependent electrode/electrolyte interfacial potential drop, which could originate from various phenomena. Hence, the total thermo-voltage in an ionic thermoelectric supercapacitor device is:

$$\Delta V = -S\Delta T + \varphi_{(T=\text{cold})} - \varphi_{(T=\text{hot})} = -S\Delta T + \Delta\varphi(\Delta T) \quad (3)$$

where $\varphi_{(T=\text{cold})}$ and $\varphi_{(T=\text{hot})}$ are the electrode/electrolyte potential drops at the hot and cold sides, respectively. It is most likely that those two terms depend on each other since both affect the concentration of ions at the electrode vicinity, but for the sake of simplicity we assume them independent.

Considering the dynamics of the thermo-voltage can be a way to distinguish between those effects. Indeed, the time constant of ionic thermodiffusion increases quadratically with the diffusing distance ($\tau \sim L^2/D$),^[18] while the time dependence of the interfacial effect $\Delta\varphi(\Delta T)$ should not depend on the distance

between the electrodes. **Figure 4** displays the time evolution of the thermo-voltage of devices composed of the same electrodes (PEDOT:PSS mixed with 3% DMSO) with short (1 mm) and long (15 mm) electrodes separations. When the electrodes are close to each other, there is only a short delay between the temperature evolution (black curve) and the thermo-voltage (red curve in Figure 4a). For the long electrode separation distance, the saturation for the thermo-voltage under similar temperature difference takes a longer time due to the slow ionic thermodiffusion (Figure 4b). Figure 4c summarizes the generated thermo-voltage from both short and long devices at different temperature difference from 1.6 to 15 K. The measured thermo-voltage is larger for long-separated devices than that for short-separated one. This can be attributed to the opposite sign between the ionic thermodiffusion induced voltage in the electrolyte and the difference in interfacial voltage at the electrodes. The ionic Soret induced effect on the thermo-voltage in the IL-p gel at steady state is expected to be similar for the same temperature gradient irrespective of the distance between the electrodes. Hence, the fact there is a large difference between the short and long distance indicates that either the steady state is not reached or there are interplays between the interfacial effect and the Soret effect. Non ideal thermoelectric effect is also clearly visible in Figure 4 because the thermo-voltages do not increase linearly with ΔT indicating more complex phenomena come into play.

Our hypothesis is that for PEDOT:PSS electrodes, the electrode/electrolyte potential drop largely originates from the Donnan exclusion (ϕ_D) of the anions of the IL induced by the PSS polyanions in the PEDOT:PSS electrodes. This is possible

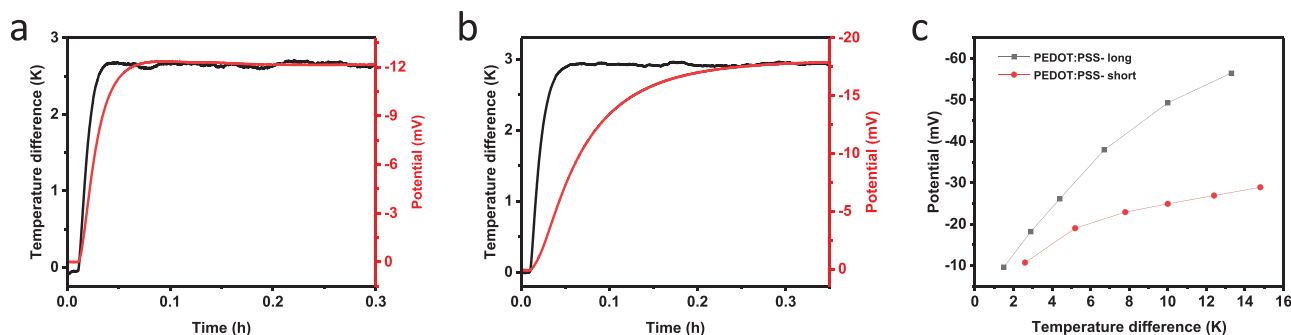


Figure 4. The thermo-voltage of devices with different separation between the two electrodes. a) The evolution of the thermo-voltage when electrodes are separated by 1 mm and b) by 15 mm. c) the thermo-voltage increasing with temperature difference for both devices.

due to the relatively low concentration of mobile ions in the IL (95% of ions pairs acting as a neutral solvent):

$$\varphi_D(T) = \frac{RT}{nF} \ln \frac{[\text{anion}]_{\text{in}}}{[\text{anion}]_{\text{out}}} \quad (4)$$

Where R is the gas constant, T is the absolute temperature of the electrodes, n is the number of charges carried by the ions, F is the Faraday constant, and $[\text{anion}]_{\text{in}}$ and $[\text{anion}]_{\text{out}}$ represent the concentration of the TFSI anion inside the electrode and outside the electrode (i.e., in the IL-p gel electrolyte), respectively. Now, the thermo-voltage from an ITESC composed of PEDOT:PSS electrodes will be expressed as:

$$\Delta V = -S\Delta T + \Delta\varphi(\Delta T) = -S\Delta T + \frac{RT_{\text{hot}}}{nF} \ln \left(\frac{[\text{anion}]_{\text{in}}^{\text{hot}}}{[\text{anion}]_{\text{out}}^{\text{hot}}} \right) - \frac{RT_{\text{cold}}}{nF} \ln \left(\frac{[\text{anion}]_{\text{in}}^{\text{cold}}}{[\text{anion}]_{\text{out}}^{\text{cold}}} \right) \quad (5)$$

Rigorous expression must be complicated as the anion concentration at different temperature is interdependent on the Soret effect. If we neglect this interplay and assume the anionic exclusion effect independent on the temperature, which is likely correct for small ΔT , then $[\text{anion}]_{\text{out}}^{\text{hot}} = [\text{anion}]_{\text{out}}^{\text{cold}}$ and $[\text{anion}]_{\text{in}}^{\text{hot}} = [\text{anion}]_{\text{in}}^{\text{cold}}$, which simplifies in:

$$\frac{\Delta V}{\Delta T} = \frac{R}{nF} \ln \frac{[\text{anion}]_{\text{in}}}{[\text{anion}]_{\text{out}}} - S \quad (6)$$

the first term $\varphi_D(T) = \frac{RT}{nF} \ln \frac{[\text{anion}]_{\text{in}}}{[\text{anion}]_{\text{out}}}$ becomes large for

PSS/Au and negligible for PEDOT:Tos. For small ΔT , Figure 2a indeed displays a rather linear evolution of ΔV versus ΔT with various slope depending on the PSS content.

As a final discussion, to evaluate the energy conversion efficiency of ionic thermoelectric device based on PEDOT electrodes, ZT factor can be calculated from Equation (1). With the effective thermopower of -3.8 mV K^{-1} , the ionic conductivity of 2.34 mS cm^{-1} , and the thermal conductivity of $0.136 \text{ W m}^{-1} \text{ K}^{-1}$, of IL-p gel, the resulting ZT value is 0.073. This is a decent value for an n-type ionic thermoelectric material. Moreover, for

practical applications the stored energy during the charging should be considered. According to Equation (2) the stored energy at the temperature difference of 1 K per area would be 60.6 nJ cm^{-2} .

3. Conclusion

In summary, we experimentally demonstrated the contribution of interfacial phenomena with conducting polymer PEDOT electrodes to the thermoelectric performance of iTE devices. PEDOT-based electrodes with gradually varying PSS content were used in ITESCs with IL-p gel as the electrolytes. The thermo-induced voltage coefficient $\Delta V/\Delta T$ of the ITESCs increased when higher PSS contents was added in the electrodes. We can conclude that the potential at PEDOT:PSS electrode/electrolyte interface triggered by a Donnan-like exclusion effect that causes a concentration difference of the anion inside and outside the electrode. Upon the temperature difference, the interfacial potential differs and contributes to the thermo-voltage in conjunction with the ionic Seebeck effect of the electrolyte. Our study emphasizes the important role of the interfacial potential for the design of ionic thermoelectric supercapacitors with conducting polymer electrodes. These findings are of key importance to understand and optimize interfacial properties of polymers and electrolytes, which are crucial for many organic electrochemical devices. Moreover, our results show that PEDOT:PSS is highly suitable to be used as electrode in ionic thermoelectric energy harvesting devices without any current collector.

4. Experimental Section

Preparation and Characterization of Electrodes: The commercial aqueous dispersion of PEDOT:PSS (CLEVIOS PH 1000) including 0.1 wt% of GOPS were mixed with DMSO (Sigma-Aldrich) at different volume ratio (0.1%, 0.5%, 1%, 3%, and 5% v/v). The solutions were stirred for few hours at room temperature. For fabrication of planar devices, the substrates were patterned by kapton tape. The PEDOT electrodes were prepared by drop casting of the solutions on patterned glass substrates. Finally, the films were annealed at $140 \text{ }^\circ\text{C}$ for 30 min on a hot plate.

For the post-treated samples, the PEDOT:PSS electrodes without GOPS were immersed into the various solvents, DMSO, Methanol (Sigma-Aldrich) and 95 wt% H_2SO_4 (Sigma-Aldrich) for 1 h at ambient

environment. Then, the electrodes were sufficiently washed in deionized water to remove residual solvents. Then, they were annealed like the former electrodes. To conduct UV–Vis spectroscopy measurements, the PEDOT:PSS films (≈ 200 nm) were prepared by spin coating the PEDOT:PSS solution onto quartz substrates by following the same post-treatment process as described before.

For the preparation of PEDOT:tosylate (PEDOT:Tos) films, 3,4-ethylenedioxythiophene (EDOT), pyridine and n-butanol were purchased by Sigma Aldrich, while iron toluenesulfonate solutions were purchased by Heraeus (Clevios B54). PEDOT:Tos was polymerized following the procedure reported elsewhere.^[33] To fabricate the PSSH/Au electrodes, the solution of commercial PSSH was diluted with water and the 0.1 wt% GOPS was added to make a similar suspension of PH1000 without PEDOT chains. Then, the electrodes were deposited on the stripes of gold and annealed similar to PEDOT:PSS electrodes. The thickness of all samples was measured with profilometer (Dektak). The thicknesses of different samples were in the range of 1 to 2 μm . The sheet resistance measured via the four-point probe technique. The electrical conductivity was obtained by inverse of multiplication of sheet resistance and thickness.

Fabrication and Characterization of Devices: The preparation strategy of ion gel was reported in the last publication.^[16] Briefly, it was prepared by mixing IL ([EMIM][TFSI]) and acetone solution of co-polymer (PVDF-HFP, $W_{\text{polymer}}/W_{\text{acetone}} = 1:7$) with the ratio of four for IL/PVDF-HFP. The ion gel was drop-casted on a micro-slide, dried in 60 °C on hot plate for 15 min. To evaluate the effect of the current collector, two narrow Au lines were evaporated on the glass and the similar process were repeated for making the PEDOT electrodes on the top of the Au electrodes.

The thermo-voltage measurements were carried out using a home-made set up at ambient environment. The temperature difference (ΔT) across the sample's surface was applied a pair of Peltier element. The open circuit voltage (V_{oc}) through the sample was recorded by a nanovoltmeter (Keithley Instruments, Inc., model 1282 A). The effective thermopower, S_{eff} , were estimated by considering the slope of the linear $V_{oc}-\Delta T$ curve. The electrochemical measurements were carried out at room temperature using potentiostat (Biologic SP-200 potentiostat) in a two electrodes configuration. For electrochemical characterizations, the sandwich structure device were fabricated, which contained two PEDOT:PSS electrodes with electrolyte between them (the thickness of electrolyte was about 1 mm). The cyclic voltammetry (CV) was carried out at the scan rate (s) of 20 mV s^{-1} and in the potential range (ΔV) of 0 to 0.2 V.

The galvanostatic charge-discharge (GCD) measurements were conducted within the same potential window at different current densities. The areal capacitance (C_A) was obtained from the GCD curve based on the following equation:

$$C_A = \frac{I_d}{dV/dt} \quad (7)$$

where I_d and dV/dt are the discharge current density (mA cm^{-2}) and the average derivative of the discharge potential, respectively.

The electrochemical impedance spectroscopy data (EIS) were measured using an ac voltage amplitude of 10 mV while sweeping the frequency from 1×10^5 to 1×10^{-2} Hz. The ionic conductivity is obtained from

$$\sigma = \frac{L}{Z'A} \quad (8)$$

where L is the distance between the two electrodes, Z' is the real part of impedance when the phase angle goes to zero, and A is the area of the electrodes.

Supporting Information

Supporting Information is available from the Wiley Online Library or from the author.

Acknowledgements

This work was financially supported by the Swedish Government Strategic Research Area in Materials Science on Advanced Functional Materials at Linköping University (Faculty Grant SFO-Mat-LiU No. 2009-00971), the Knut and Alice Wallenberg Foundation (Tail of the sun), the Swedish Research Council (grant No. 2016–05990, 2016–06146, 2020–05218, and 2018–04037).

Conflict of Interest

The authors declare no conflict of interest.

Data Availability Statement

The data that supports the findings of this study are available in the supplementary material of this article.

Keywords

interface electrode-electrolyte, ionic thermoelectrics, supercapacitors, Soret effect, supercapacitors

Received: May 17, 2021

Revised: July 26, 2021

Published online:

- [1] G. J. Snyder, E. S. Toberer, *Nat. Mater.* **2008**, *7*, 105.
- [2] A. S. Rattner, S. Garimella, *Energy* **2011**, *36*, 6172.
- [3] N. Toshima, *Synth. Met.* **2017**, *225*, 3.
- [4] B. Saleh, G. Koglbauer, M. Wendland, J. Fischer, *Energy* **2007**, *32*, 1210.
- [5] A. P. Straub, M. Elimelech, *Environ. Sci. Technol.* **2017**, *51*, 12925.
- [6] D. Champier, *Energy Convers. Manage.* **2017**, *140*, 167.
- [7] S. Mardi, M. Pea, A. Notargiacomo, N. Yaghoobi Nia, A. Di Carlo, A. Reale, *Materials* **2020**, *13*, 1404.
- [8] K. Wijeratne, U. Ail, R. Brooke, M. Vagin, X. Liu, M. Fahlman, X. Crispin, *Proc. Natl. Acad. Sci. USA* **2018**, *115*, 11899.
- [9] D. Zhao, H. Wang, Z. U. Khan, J. C. Chen, R. Gabrielsson, M. P. Jonsson, M. Berggren, X. Crispin, *Energy Environ. Sci.* **2016**, *9*, 1450.
- [10] M. Bonetti, S. Nakamae, M. Roger, P. Guenoun, *J. Chem. Phys.* **2011**, *134*, 114513.
- [11] T. Li, X. Zhang, S. D. Lacey, R. Mi, X. Zhao, F. Jiang, J. Song, Z. Liu, G. Chen, J. Dai, *Nat. Mater.* **2019**, *18*, 608.
- [12] H. Cheng, X. He, Z. Fan, J. Ouyang, *Adv. Energy Mater.* **2019**, *9*, 1901085.
- [13] J. Wang, S.-P. Feng, Y. Yang, N. Y. Hau, M. Munro, E. Ferreira-Yang, G. Chen, *Nano Lett.* **2015**, *15*, 5784.
- [14] H. Wang, D. Zhao, Z. U. Khan, S. Puzinas, M. P. Jonsson, M. Berggren, X. Crispin, *Adv. Electron. Mater.* **2017**, *3*, 1700013.
- [15] S. Horike, Q. Wei, K. Kirihaara, M. Mukaida, T. Sasaki, Y. Koshiha, T. Fukushima, K. Ishida, *ACS Appl. Mater. Interfaces* **2020**, *12*, 43674.
- [16] D. Zhao, A. Martinelli, A. Willfahrt, T. Fischer, D. Bernin, Z. U. Khan, M. Shahi, J. Brill, M. P. Jonsson, S. Fabiano, *Nat. Commun.* **2019**, *10*, 1093.
- [17] B. Kim, J. U. Hwang, E. Kim, *Energy Environ. Sci.* **2020**, *13*, 859.
- [18] M. Bonetti, S. Nakamae, B. T. Huang, T. J. Salez, C. Wiertel-Gasquet, M. Roger, *J. Chem. Phys.* **2015**, *142*, 244708.
- [19] H. Lim, W. Lu, X. Chen, Y. Qiao, *Nanotechnology* **2013**, *24*, 465401.

- [20] N. Kim, I. Petsagkourakis, S. Chen, M. Berggren, X. Crispin, M. P. Jonsson, I. Zozoulenko, *Conjugated Polymers: Properties, Processing, and Applications*, CRC Press, Boca Raton, FL **2019**.
- [21] M. Berggren, X. Crispin, S. Fabiano, M. P. Jonsson, D. T. Simon, E. Stavrinidou, K. Tybrandt, I. Zozoulenko, *Adv. Mater.* **2019**, *31*, 1805813.
- [22] K. Sun, S. Zhang, P. Li, Y. Xia, X. Zhang, D. Du, F. H. Isikgor, J. Ouyang, *J. Mater. Sci.: Mater. Electron.* **2015**, *26*, 4438.
- [23] S. L. Kim, H. T. Lin, C. Yu, *Adv. Energy Mater.* **2016**, *6*, 1600546.
- [24] X. Wu, B. Huang, Q. Wang, Y. Wang, *Chem. Eng. J.* **2019**, *373*, 493.
- [25] A. Håkansson, S. Han, S. Wang, J. Lu, S. Braun, M. Fahlman, M. Berggren, X. Crispin, S. Fabiano, *J. Polym. Sci., Part B: Polym. Phys.* **2017**, *55*, 814.
- [26] H. Shi, C. Liu, Q. Jiang, J. Xu, *Adv. Electron. Mater.* **2015**, *1*, 1500017.
- [27] Z. U. Khan, O. Bubnova, M. J. Jafari, R. Brooke, X. Liu, R. Gabrielsson, T. Ederth, D. R. Evans, J. W. Andreasen, M. Fahlman, *J. Mater. Chem. C* **2015**, *3*, 10616.
- [28] J. Zhang, Y. Zhao, C.-G. Yuan, L.-N. Ji, X.-D. Yu, F.-B. Wang, K. Wang, X.-H. Xia, *Langmuir* **2014**, *30*, 10127.
- [29] D. Alemu, H.-Y. Wei, K.-C. Ho, C.-W. Chu, *Energy Environ. Sci.* **2012**, *5*, 9662.
- [30] S. Mardi, O. Moradlou, A. Z. Moshfegh, *J. Solid State Electrochem.* **2018**, *22*, 3507.
- [31] J. Luo, D. Billep, T. Waechter, T. Otto, M. Toader, O. Gordan, E. Sheremet, J. Martin, M. Hietschold, D. R. T. Zahn, T. Gessner, *J. Mater. Chem. A* **2013**, *1*, 7576.
- [32] N. Kim, S. Kee, S. H. Lee, B. H. Lee, Y. H. Kahng, Y. R. Jo, B. J. Kim, K. Lee, *Adv. Mater.* **2014**, *26*, 2268.
- [33] I. Petsagkourakis, E. Pavlopoulou, E. Cloutet, Y. F. Chen, X. Liu, M. Fahlman, M. Berggren, X. Crispin, S. Dilhaire, G. Fleury, *Org. Electron.* **2018**, *52*, 335.